

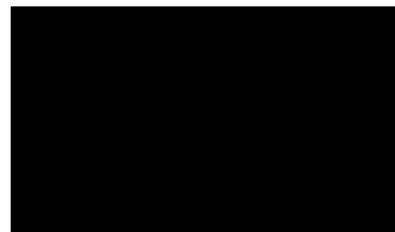
**FLOW EXCURSION EXPERIMENTS WITH A PRODUCTION
REACTOR ASSEMBLY MOCKUP (U)**

by

C. A. Nash, G. C. Rush, and J. E. Blake

Westinghouse Savannah River Company
Savannah River Site
Aiken, South Carolina 29808

A paper proposed for presentation and publication at
*The Safety, Status, and Future of Commercial
Reactors and Irradiation Facilities Meeting*
Boise, Idaho
September 30-October 4, 1990



This paper was prepared in connection with work done under Contract No. DE-ACO9-89SR18035 with the U.S. Department of Energy. By acceptance of this paper, the publisher and/or recipient acknowledges the U.S. Government's right to retain a nonexclusive, royalty-free license in and to any copyright covering this paper, along with the right to reproduce and to authorize others to reproduce all or part of the copyrighted paper.

FLOW EXCURSION EXPERIMENTS WITH A PRODUCTION REACTOR ASSEMBLY MOCKUP

G. C. Rush and J. E. Blake
Babcock & Wilcox Company
Alliance, OH 44601
(216) 829-7397

C. A. Nash
Westinghouse Savannah River Company
Savannah River Site
Aiken, SC 29808
(803) 725-2827

ABSTRACT

A series of power ramp and loss-of-coolant accidents were simulated with an electrically heated mockup of a Savannah River Site production reactor assembly. The one-to-one scale mockup had full multichannel annular geometry in its heated section in addition to prototypical inlet and outlet endfitting hardware. Power levels causing void generation and flow instability in the water coolant flowing through the mockup were found under different transient and quasi-steady state test conditions. A reasonably sharp boundary between initial operating powers leading to or not leading to flow instability were found: that being 0.2 MW or less on power levels of 4 to 6.3 MW. Void generation occurred before, but close to, the point of flow instability. The data were taken in support of the Savannah River reactor limits program and will be used in continuing code benchmarking efforts.

INTRODUCTION

A novel, full-scale, nuclear reactor fuel assembly mockup was used to study the transient thermal-hydraulic response of the mockup during postulated Savannah River Site (SRS) nuclear reactor accidents. The electrically heated mockup was constructed to simulate the unique annular concentric-tube geometry of the fuel assemblies in SRS production reactors. Several major design challenges were overcome to yield a mockup fuel assembly that closely replicated the prototypical thermal-hydraulic channel geometry. A balance of test facility hardware arrangement provided the needed flexibility to impose a variety of time-dependent pressure boundary conditions across the fuel assembly during the accident simulations. Tests performed over a power range from 2 to 6.3 MW and with varying time dependent pressure boundary conditions produced static flow instabilities (Ledinegg¹). The instrumentation set was used to measure the transient fluid and heater tube metal temperatures, assembly flow rate, channel exit dynamic pressure as sensed by in-channel Pitot tubes, and channel exit void fraction measured by fiber optic void probes.

Ledinegg¹ flow instability is an important concern in setting SRS reactor power limits because it can lead to fuel dryout followed by rapid fuel temperature excursion and damage. Previous experimental work that examined flow instability in a downflow arrangement involved simpler geometries^{2,3} than the subject work and produced demand curves (characteristic flow versus pressure drop relationships up to flow instability) that were generated under quasi-steady conditions. The data from the subject work will be used as a benchmark for the predictive performance and governing thermal-hydraulic models of plant-predictive computer codes at near prototypic operating conditions. Reactor heat transfer correlations from the commercial nuclear industry were generally not applicable to the subject work because of the unique SRS fuel assembly geometry. In addition, the low operating pressure of 138 to 690 kPa (20 to 100 psia) and reactor outlet temperature of less than 150°C (302°F) were substantially below those of the commercial plants. Hence, full-scale tests like those described herein were needed by the SRS.

The primary focus of the subject experimental program was the Double-Ended Guillotine Break (DEGB) in one of the six inlet coolant lines of the reactor inlet plenum. Mockup fuel assembly heater power and time-dependent inlet and outlet plenum pressure profiles simulated the best-estimate calculations of the design basis Loss-Of-Coolant Accident (LOCA). The tests established the power threshold above which flow instability during the transient would be expected.

This paper presents an overall summary of the test program. The hardware of the mockup fuel assembly and test facility are outlined. The fuel assembly instrumentation and test boundary condition controls are described. A summary of overall results from the completed LOCA and power ramp test program is presented.

MOCKUP FUEL ASSEMBLY

The mockup fuel assembly consisted of both prototypic and test manufactured components. The mockup fuel assembly shown in Figure 1 replicated the prototypic fuel assembly in many respects. The electrically heated mockup, tested at power levels to 6.3 MW, preserved the full-length, concentric fuel and target tube arrangement present in the prototype. Prototypic channel-to-channel flow splits were closely preserved. This was accomplished through detailed hydraulic scaling considerations. (The channel geometry was necessarily distorted because of the aprototypic heater tube wall thickness and rib size.) Tight machining tolerances (wall tolerances of ± 0.025 mm) and assembly tolerances of the fuel assembly internal parts were also adhered to. Power splits between the inner and outer heater tubes (52 and 48% respectively) matched the design target. The specified chopped-cosine axial power profile, with a peak-to-average power ratio of 1.3, was approximated using 0.279-m (11-in.) tapered tube sections and material variations along the heated length. Target tubes were 6061-T6 aluminum and also machined in 0.279-m lengths to facilitate assembly. Ceramic ribs provided electrical isolation between the heater and target tubes and preserved the prototypic subchannel geometry.

Use of the prototypic universal sleeve housing confined the overall mockup fuel assembly diameter to prototypic dimensions. Actual bottom and top fitting hardware was used where feasible. The monitor pin at the bottom of the endfitting was machined to prototypic dimensions and instrumented in a prototypic manner for temperature and pressure.

The heater design evolved to a resistively heated, single-wall tube to achieve the chopped-cosine power profile and the design peak heat flux of 3.2 MW/m^2 ($1.1\text{E}+6 \text{ Btu/hr-ft}^2$). Because of the power supply characteristics (10 MW at 50,000 amps and 200 volts DC), close machining tolerances, assembly constraints, and readily available materials, the simulated fuel tubes (mockup heater tubes) consisted of tapered wall, 0.279-m (11-in.) segments that were custom welded (TIG or electron beam) or vacuum-furnace brazed to yield the full length heated tube. Use of Monel 400 along the length of the inner and outer heater tubes, except for the 0.41-m (16-in.) ends, yielded wall thickness at mid-length (and peak heat flux) of 0.76 mm (0.030 in.) and 1.04 mm (0.041 in.) for the outer and inner heater tubes, respectively. The end piece transition to the massive copper electrical bus bar connectors was completed with 70-30 and 90-10 copper-nickel tube sections.

Because of the thin-wall tube design and high-current input (about 40,000 amps at 6 MW), the heater tubes were not strong enough to support the weight of the upper electrical connector (Figure 1) nor the compressive loading that would develop during transient temperature excursions without buckling. To preclude heater tube buckling and maintain the tubes in tension during steady state and transient operation, a novel tensioner assembly was coupled to the upper electrical connector. The tensioner design accommodated up to one inch of differential thermal expansion between either of the two heater tubes relative to each other or to the rest of the fuel assembly.

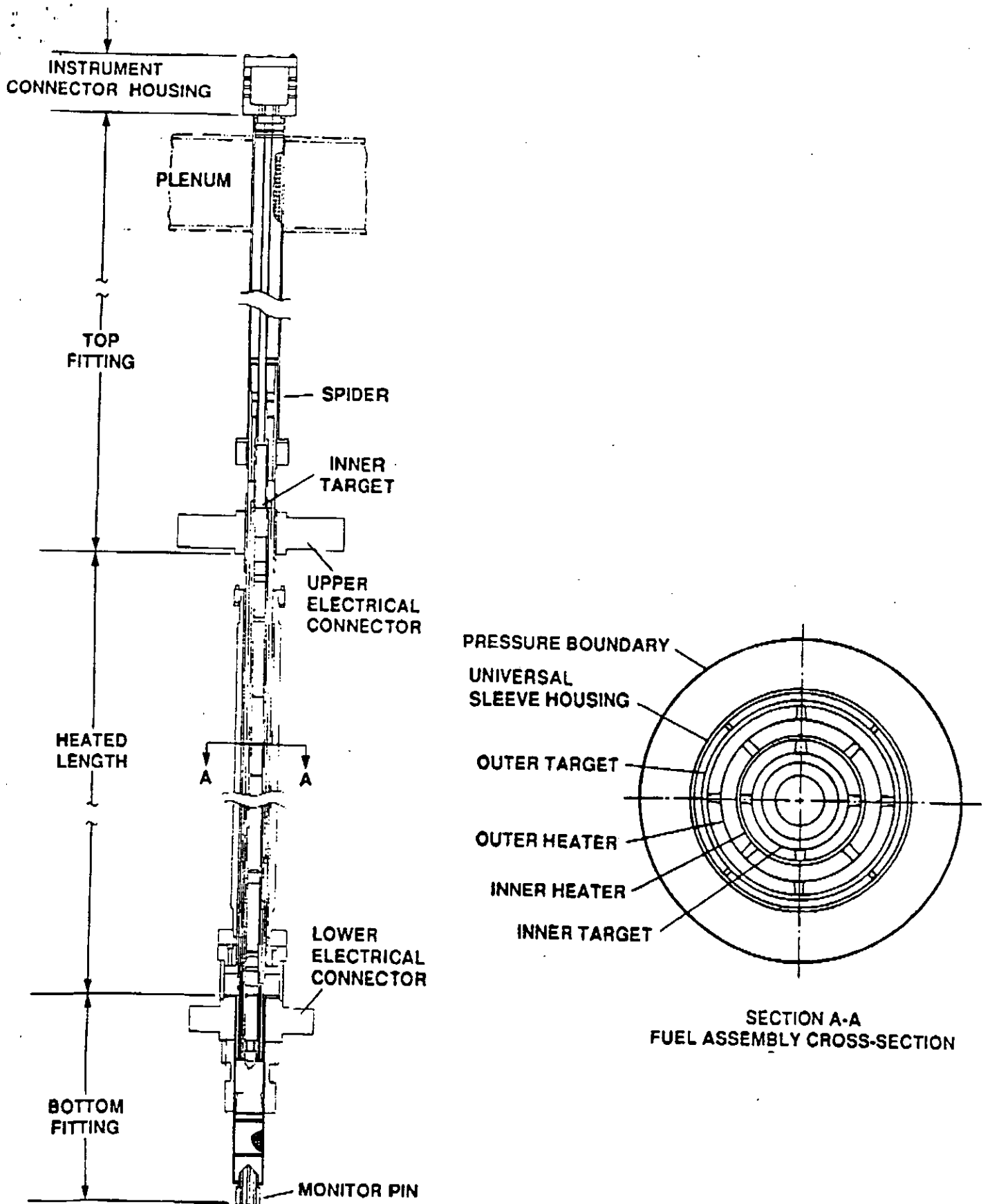


Figure 1. Mark 22 Model Fuel Assembly Schematic

Test Facility

The Flow Excursion Test Facility utilized a once-through coolant flow design for the 60-second test transient to preclude the need for large heat exchanger capacity (design basis of 7 MW) at the low exit temperatures (less than 120°C) associated with this test. The test facility is isometrically illustrated in Figure 2 and schematically shown, including the water supply, in Figure 3. During the test performance, the test loop assumed two configurations. The first configuration supported test initiation at steady state and the second implemented the test transient. The features of the test facility are described in the following text by examining the test facility operation under steady state and transient test conditions.

A 12,500 gallon reservoir associated with this flow loop supplied the needed water inventory for the test transient. During steady state facility operation, water flow in excess of 2000 gpm circulated through one of the supply pumps shown in Figure 3 and returned to the reservoir. From this recirculating flow, a bypass flow of nominally 345 gpm was controlled to the fuel assembly by valve WSCV01 shown in Figure 3. The flow was directed through the water-filled inlet reservoir to the inlet plenum through three feeder lines, each with a venturi for transient flow rate measurement, through the fuel assembly, and out to the outlet plenum and into the holding tank. The inlet plenum consisted of six permanent sleeve mockups of prototypic size and spacing with the center sleeve aligning the test fuel assembly. The outside holding tank was open to atmosphere for power dissipation of the fuel assembly effluent. With the flow conditions established, power to the fuel assembly was activated and linearly ramped to test initial conditions at a rate of about 1.5 MW per minute. The holding tank control valve, WCCV01, maintained back pressure control on the fuel assembly during test setup. The 1200-gallon inlet reservoir served as the water supply to the fuel assembly during the test transient. The 300-gallon quench tank used for energy dissipation during the test transient was water solid. The 900-gallon collection tank was nitrogen filled and pressurized to the post-accident reactor tank pressure. The pressure control system for the inlet plenum was activated at the post-accident control pressure.

The test transient was activated by a sequence of valve opening and closings that isolated the forced flow (closure of valve WSQV01) provided to the inlet reservoir. The outlet, or reactor tank pressure boundary condition, was activated by simultaneously closing WCQV01 (stopping flow to the holding tank) and opening valve WCQV02, which diverted the flow from the holding tank to the quench tank. Reactor tank pressure control was maintained by pressure-regulated nitrogen venting from the collection tank as water flowed into this tank. The inlet plenum pressure boundary condition was established by a regulated nitrogen addition to the top of the inlet reservoir, thereby precluding gas entrainment and transport through the fuel assembly. In both the reactor tank and inlet plenum pressure controls, pilot regulators were used at each location to provide a control signal to "slave" regulators that controlled the gas flow (or vent) to maintain the post-accident boundary conditions. The DEGB LOCA discussion of results describes a typical pressure trace for the inlet plenum and reactor tank, or outlet, during the nominal accident transient. The power transient followed a prescribed reactor "scram" power decay. The power and hydraulic transients were synchronized so that the substantial power drop occurred about one second after the pressure transient.

Instrumentation

A total of 94 instruments were installed in the fuel assembly consisting of 38 metal and 18 fluid Type E thermocouples, 11 differential pressure and 19 pressure measurements, power measurements for each heater tube, and void fraction and dynamic pressure (Pitot tube) measurements for each of the three active flow channels at the exit plane of the heated length. The flow rate to the fuel assembly was measured upstream of the inlet plenum using venturi flowmeters as shown in Figure 2.

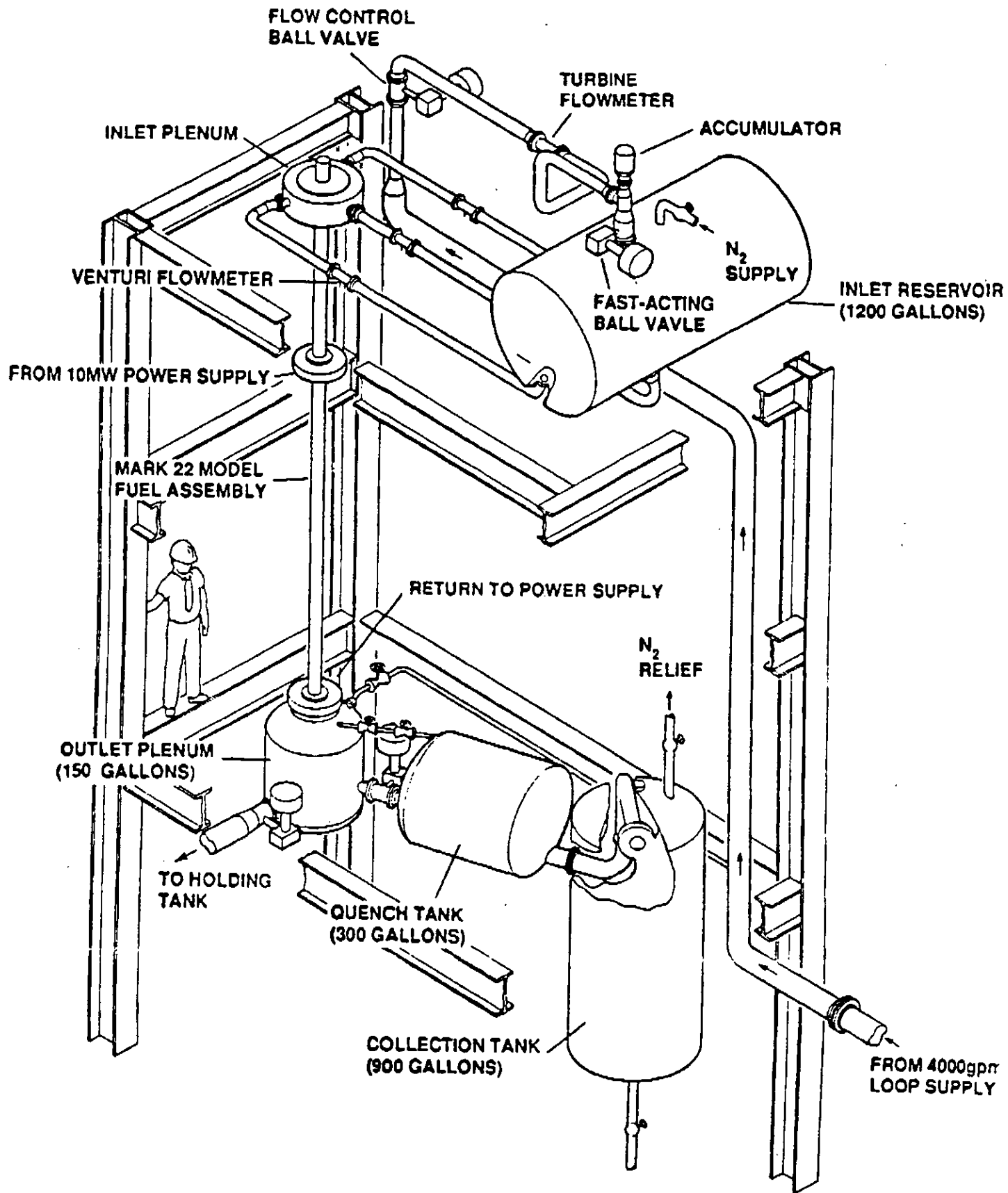


Figure 2. Test Facility

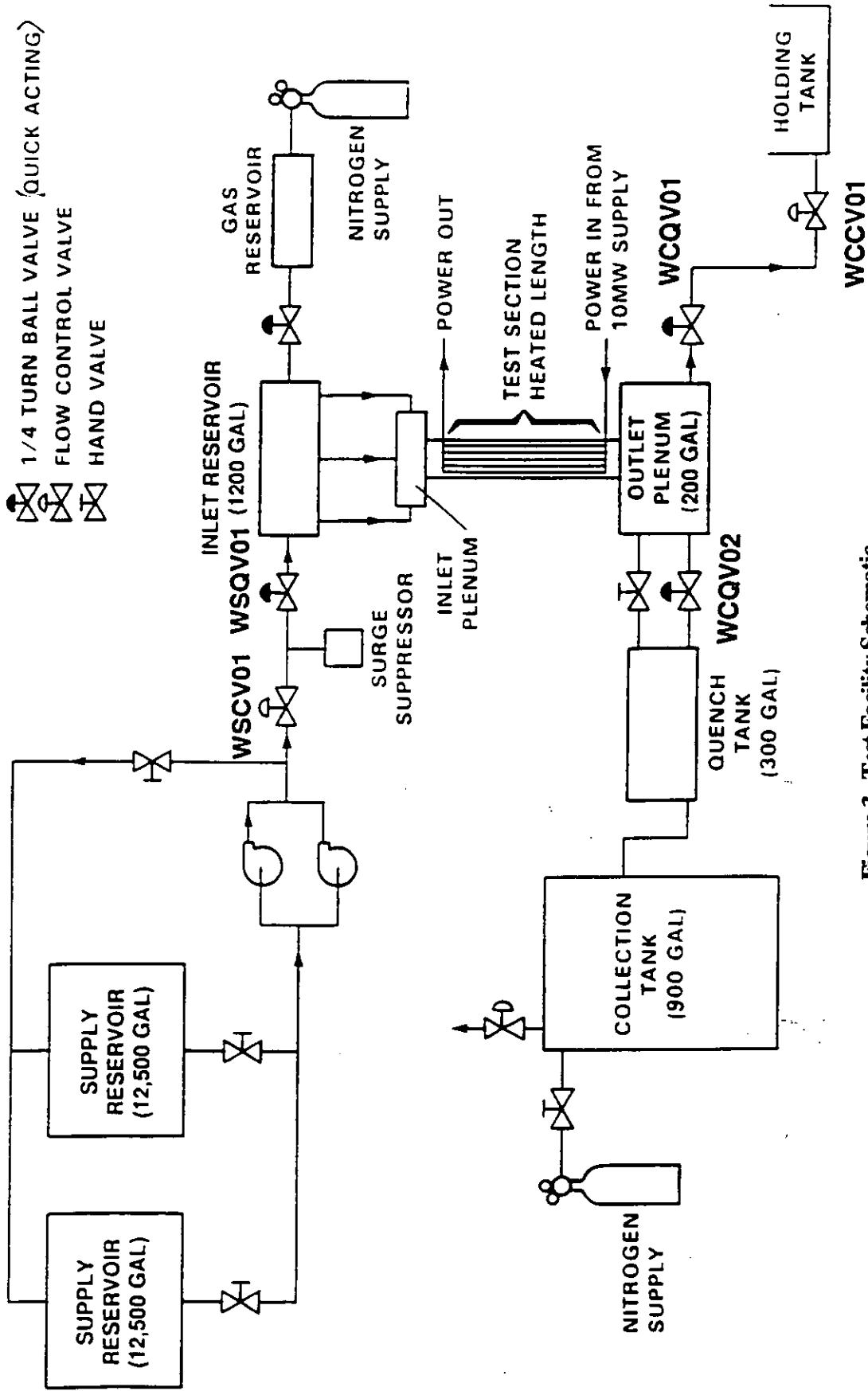


Figure 3. Test Facility Schematic

A cross-section of the fuel assembly heated section is shown in Figure 4, which illustrates a typical routing of the inner and outer heater tube thermocouples. The inner heater tube metal and fluid temperature measurements between heater tubes were routed inside the inner target tube, thereby protecting the thermocouples from the active channel flow loadings and minimizing the disturbance of the thermocouple extension wires to the heated channel flow streams.

Thermocouples from the inner target tube were routed from the inner target at the required axial elevation, inserted through a drilled hole in the inner heater (the thermocouple sheath was brazed to the heater to preclude flow leakage), and either attached to the inner heater or extended to measure the fluid temperature in the channel between the inner and outer heater tube. The outer heater tube metal and fluid thermocouples were routed within the outer heater tube ceramic ribs to preclude channel flow disturbance as shown. The rib was sized large enough to accommodate the 0.81-mm (0.032-in.) diameter thermocouples. The thermocouples were sheathed with 0.15-mm (0.006-in.) -thick wall Teflon tubes to electrically insulate the metal thermocouple sheaths from the rest of the fuel assembly. Both the inner and outer heater tube metal thermocouples were brazed into a 0.38-mm (0.015-in.) groove to bias the thermocouple temperature measurement toward that of the heater tube rather than the coolant fluid.

Pressure measurements were acquired in all of the mockup fuel assembly heated channels, including four measurements at the upper electrical connector and six measurements at the lower electrical connector. Heater design required that there be no pressure tap penetrations through the heater tubes. Because of this, channel pressure measurements were limited to overall measurements at the electrical connectors except for the heated channel between the outer heater and outer target. In this instance, six additional pressure measurements were acquired at three equally spaced axial planes with two measurements at each plane, 180 degrees opposed.

A fiber optic void fraction probe⁴ was custom designed for this test program and fuel assembly geometry. The measurement used two infrared sources (a measurement beam wave length of 1300 nm and a reference beam of 835 nm) to perform the void fraction measurement in a self-compensating mode of operation. The energy transmitted to each channel passed through the fluid and was reflected and focused from the opposite channel wall by a gold-plated spherical mirror. It then returned to the optic fiber bundle for transmission to the signal processing hardware. Absorbed-versus-scattered light depended on the void fraction along the beam path. The principle of operation of this two-wavelength unit was similar to that of a steam/air fraction IR probe studied by Lahey⁵. By using shorter IR wavelengths, the present probe was able to measure liquid/vapor water fraction (void fraction) rather than steam/air fraction.

RESULTS OF TESTING

The facility and mockup were successfully operated to simulate desired flow and power transients at prototypical levels for one assembly in a reactor that experiences the hypothetical accident being studied. Data were used to determine significant thermal-hydraulic events in a mockup that is as prototypical as possible. In ongoing analysis, the data are being used to set a benchmark for predictive codes. Results of the detailed SRS code analysis are not yet available.

The following paragraphs summarize the results of the double ended guillotine break LOCA and power ramp tests. Boundary conditions for each type of test are discussed, followed by a presentation of representative data. For all LOCA simulations, time zero corresponds to the initiation of the instantaneous pipe break. For all power ramp tests, time zero is simply the beginning of a linear power ramp from a steady initial value. In all cases, time zero of the pressure and power histories of a test are coincident.

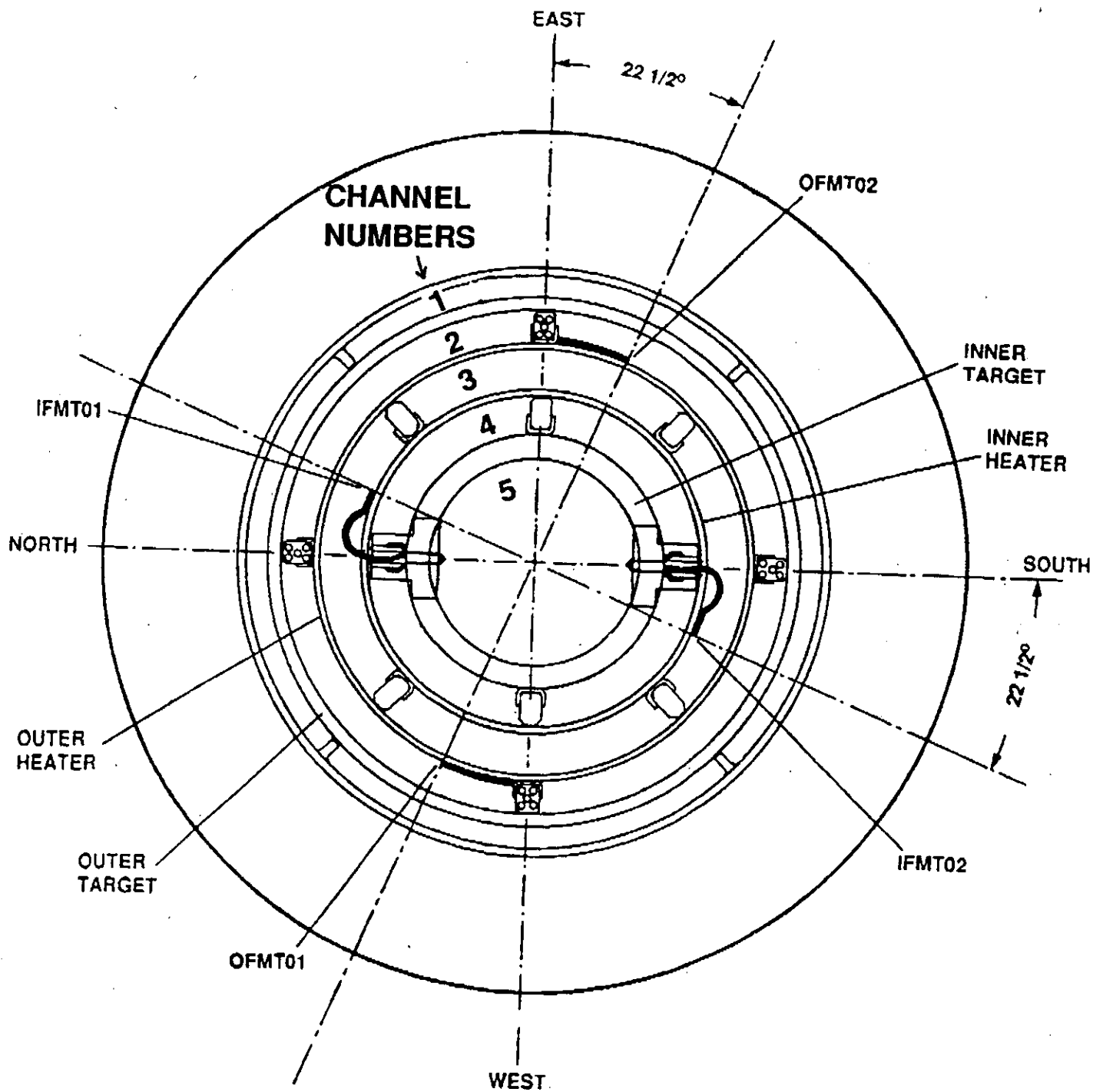


Figure 4. Fuel Assembly Cross Section Showing Thermocouple Routing

Double-Ended Guillotine Break LOCA Simulations

The DEGB LOCA accident is the limiting fault that is being considered in the SRS reactor power limits program. It is not expected to occur in reality. The acceptance criteria for the SRS methodology at this time require that reactor assemblies do not see flow instability during the limiting case accident.

One of the main purposes of the LOCA simulation test matrix was to locate the initial power at each inlet temperature that causes flow instability during the transient. This required performing a test just below and just above the power in question in order to bracket it. Table 1 presents the bracket values on initial power for Flow Instability (F1).

Boundary conditions of assembly inlet and outlet pressure and of assembly power had been calculated and were simulated in this experiment. A Transient Reactor Analysis Code (TRAC) model of the reactor was used for the coolant pressure boundary conditions. Neutronics Calculations using SRS codes AA3 and LLAP provided a power history for a reactor that scrams in response to the DEGB accident. The simulation of the pressure and power transients in the mockup facility are shown in Figures 5 and 6.

The pressure transient in Figure 5 represents the effect of a DEGB in a pipe as seen by the inlet and outlet of an SRS reactor assembly in the break sector of the reactor. The assembly operates in downflow with the higher absolute pressure applied at the top. Initial and final pressures at inlet and outlet were specified, and the initial pressure descent was as rapid as possible with the quick-acting valve setup. The substantial portion of the pressure descent was achieved in about 0.1 second. The same pressure history was used in all nominal LOCA tests.

The power history applied to the mockup represented the reactor scram response to the accident, shown as the normal power decay in Figure 6. The power remains high for about the first second as the safety rod release mechanisms in the reactor operate. A steep power descent is realized at about 1.1 seconds as safety rods fall by gravity into the core. For the latter part of the accident, the core is only producing decay heat. The calculated power response was programmed on an analog drum controller connected to the DC power supply. All nominal LOCA simulated power histories followed the same proportional curve and used a range of initial powers.

Figures 7 and 8 are examples of inlet flow response to the imposed pressure and power transients. These flow histories are of two of the LOCA tests done at 27°C inlet temperature and are the bracketing points for this inlet temperature (Figure 9). The tests were done at 5.15 and 5.23 MW, respectively, and show how sensitive that flow behavior is to initial power. Run 867_19 is judged to be a flow instability because it shows a substantial flow reduction beyond that which is caused by the simulated pipe break. Measured inlet flow dropped to zero in most tests that exhibited flow instability.

Run 867_19 was one of a few examples of recovery from flow instability that were seen during the test program. The power history for most tests was forced immediately to zero sometime between 1 and 2 seconds into the transient as a result of a low flow or high heater temperature signal detected by the safety system of the rig. The safety system shut off the power supply in those cases. While recovery during powered operation was sometimes noted, its analysis was beyond the scope of the current SRS limits methodology.

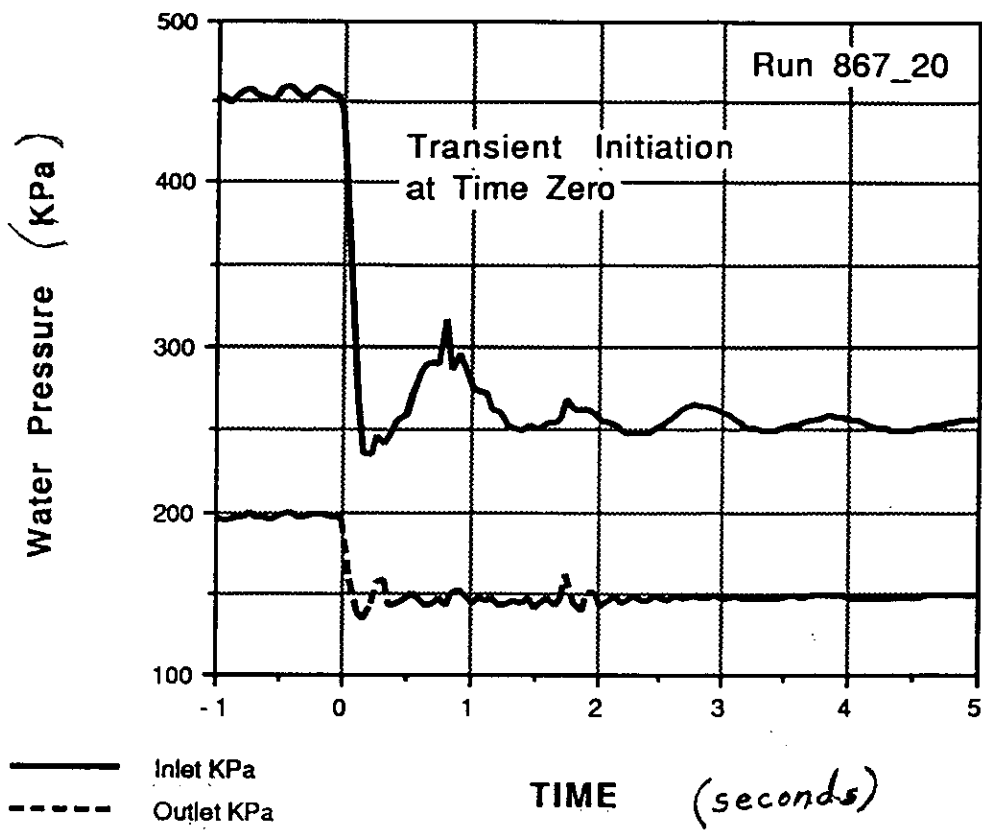


Figure 5. Imposed Pressure Transient at the Mockup Inlet and Outlet

Power decay is normalized with respect to the starting power. Power is held constant for times greater than 7 seconds.

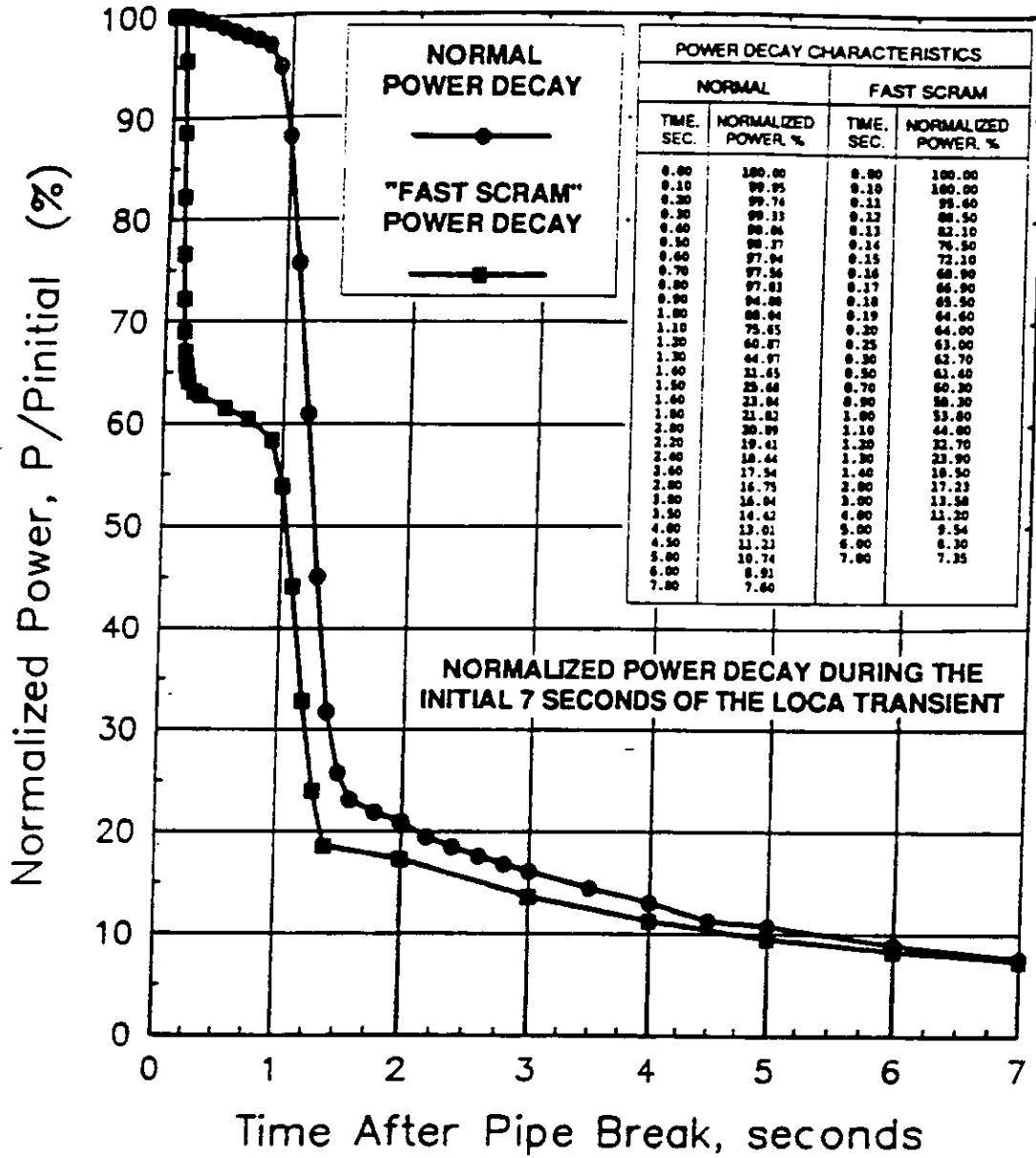


Figure 6. Nominal and Fast Scram Power Decay Curves

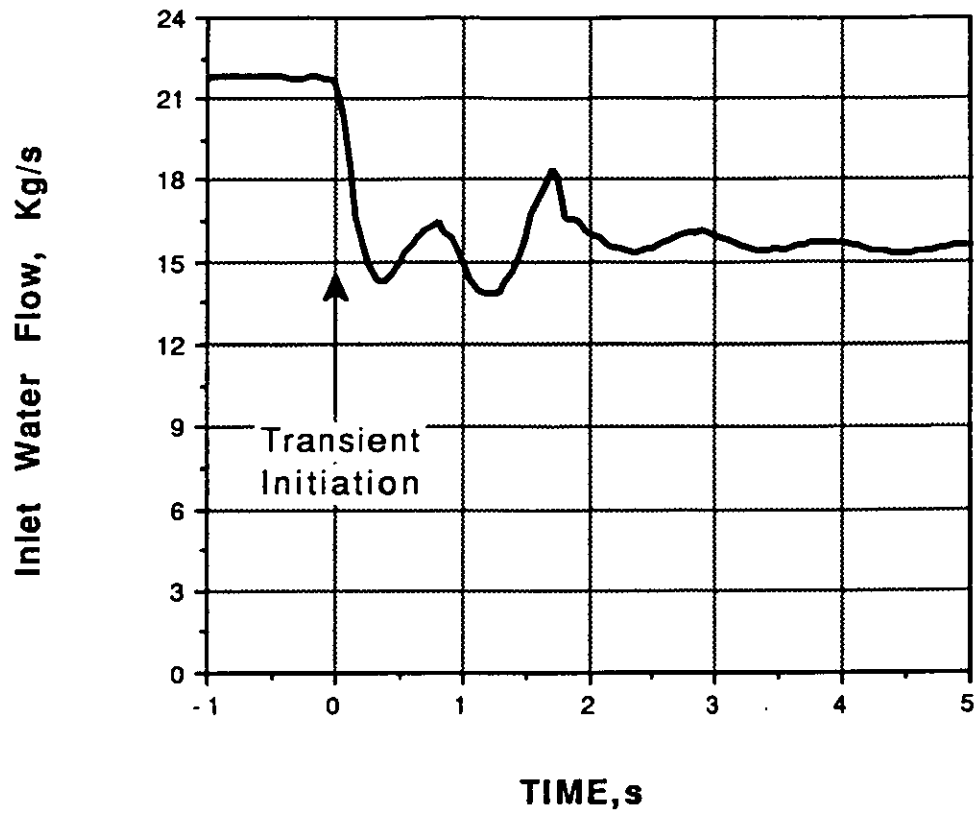


Figure 7. Run 867-20 Inlet Flow: No Flow Instability

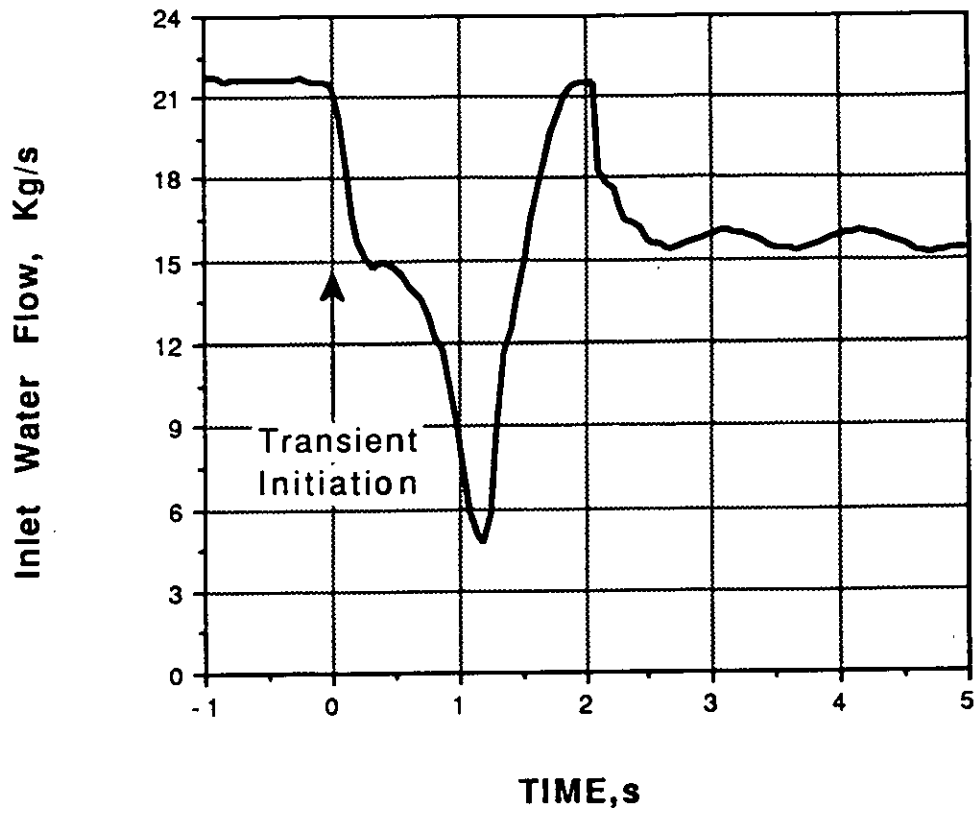


Figure 8. Run 867-19 Inlet Flow: Flow Instability

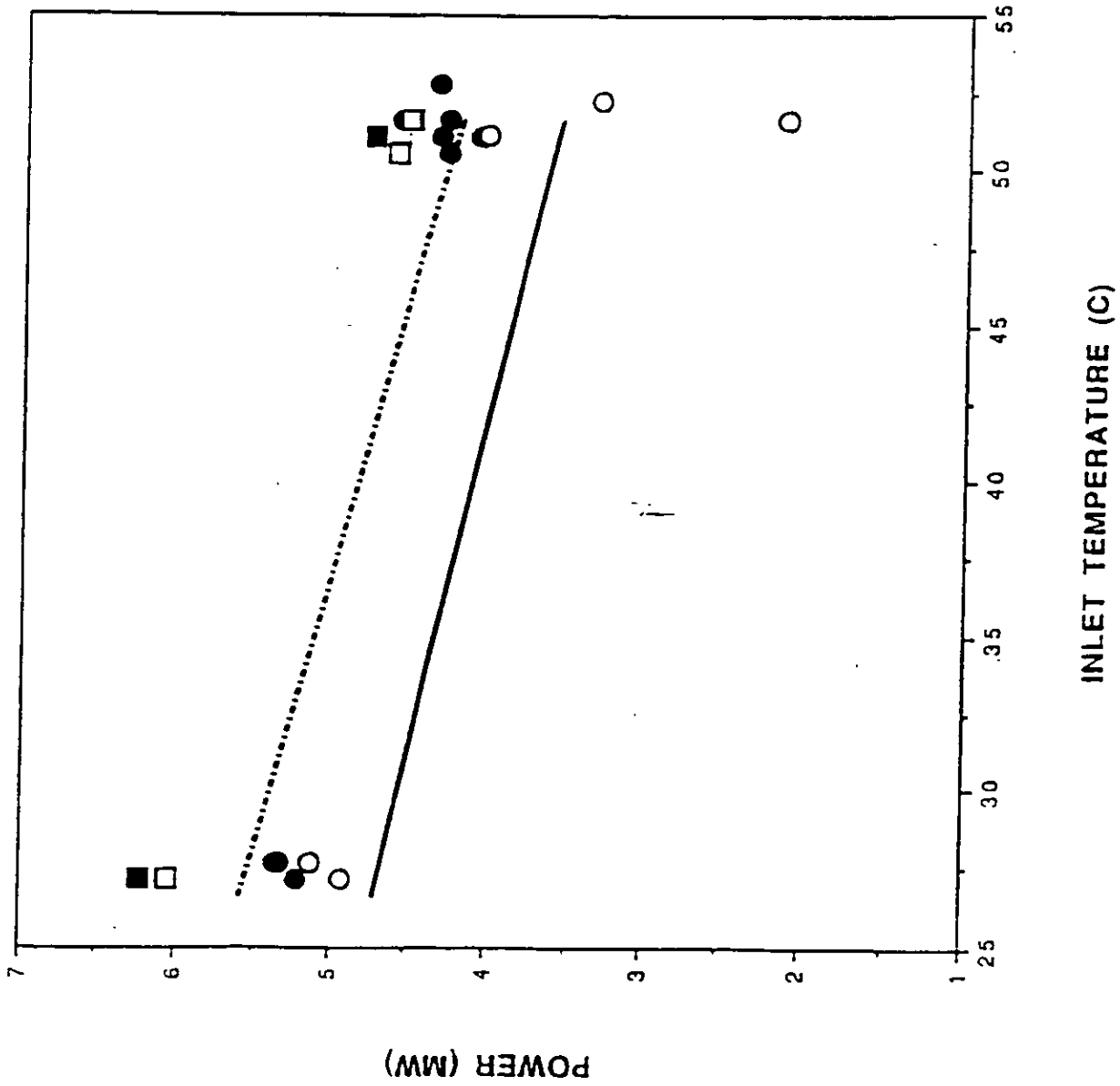


Figure 9. Reactor Assembly Mockup LOCA Test Results

Effect of a Faster Scram Power Curve

The effect of a more rapid, double-step power history on maximum initial power before flow instability was studied. The faster scram history was the calculated effect of using fast poison injection to scram the reactor. While no such systems are implemented at SRS, a simulation of their effect on power level for flow instability was of interest. It is shown as the fast scram power decay in Figure 6. The same pressure history used in the other DEGB LOCA simulations was imposed on the mockup.

Initial powers bracketing flow instability under the fast scram power history are shown in Table 1 and Figure 9. This single assembly mockup experiment did demonstrate a limiting power advantage as shown in the table. While results cannot be extended proportionally to reactor power limits, they will be useful in establishing a benchmark for the SRS thermal-hydraulic codes used in the limits methodology.

Table 1. Measured Initial Powers Bracketing Flow Instability

Power History	Inlet Temperature °C (°F)	Initial Powers Bracketing FI (MW)
Normal Scram	27 (80)	5.15 - 5.23
Normal Scram	51 (125)	4.00 - 4.10
Fast Scram	27 (80)	6.04 - 6.23
Fast Scram	51 (125)	4.60 - 4.75

Power Ramp Tests

Power ramp tests involved the gradual and linear increase of mockup heat power while pressure at the inlet and outlet of the mockup assembly was being held constant in time. Purposes of performing power ramp tests were to:

- Note the power difference between Onset of Significant Void (OSV) as indicated by channel exit void fraction probes and overall assembly Flow Instability (FI);
- Study the mockup under quasi-steady conditions as it approached flow instability to seek indications of propagation of flow instability between channels in the multichannel rig;
- Look for the possible occurrence of Critical Heat Flux (CHF) before OSV. It would be indicated in this experiment if it was a problem; and
- Observe the role of a two-phase pressure drop in the bottom endfitting as a possible initiator of flow instability.

Flow boundary conditions are listed in Table 2. Flow was set at the desired value by holding the outlet pressure constant and by varying inlet pressure. After the desired flowrate was achieved, pressure setpoints were set.

Table 2. Power Ramp Results

Test	Inlet Flow kg/s (lb/h)	Inlet Temp. °C (°F)	Outlet Pressure kPa abs. (psia)	P_v^{**} (MW)	P_{FI}^{***} (MW)	P_v / P_{FI}
01	9.61 (7.63E4)	26 (79)	196.5 (28.5)	2.74	2.82	0.972
02	10.3 (8.18E4)	27 (80)	144.8 (21.0)	2.66	2.75	0.967
03*	14.0 (1.11E5)	51 (125)	144.8 (21.0)	2.94	3.06	0.961
04	13.5 (1.07E5)	27 (80)	196.5 (28.5)	3.81	3.87	0.984
05	14.0 (1.11E5)	27 (80)	144.8 (21.0)	3.73	3.80	0.982
06	13.2 (1.05E5)	51 (125)	144.8 (21.0)	2.56	2.68	0.956
07	18.1 (1.44E5)	52 (126)	144.8 (21.0)	3.91	4.00	0.978

*Void was only seen at the Channel 3 exit (Figure 4)

** P_v = Power level where channel exit void was first seen

*** P_{FI} = Power at shutdown due to excursive instability

Power ascension followed the history shown in Figure 10, except that initial plateau power was different in some tests. Power was manually ramped to an initial level after flow was established about 120 seconds before the linear power ramp began. After the 120-second steady hold period, power was automatically ramped linearly in time at a rate of 1 MW per 60 seconds. The test was shut down when high heater temperature of low total inlet flow was seen.

Power ramp tests always ended in flow instability with no recovery seen until the electrical heater power was instantaneously shut off to zero by the rig safety system. A 10 percent drop in inlet flowrate or heater temperature exceeding 205°C generated the power trip. Figure 11 is an example of the excursive flow descent 58.5 seconds after the linear power ramp commenced. A sharp increase in inlet flow was seen after the power was shut off. This was undoubtedly caused by the collapse of the steam void that had formed in the mockup heated section during the flow instability that caused the flow descent.

Figure 12 shows the void fraction probe indications during the power ramp flow instability. (Channel numbers are provided in Figure 4.) Each probe took a chordal measurement at the exit of each major flow annulus. While this measurement occurs somewhat after the true onset of significant void in the heated section, it is the closest measurement available. The true point of net vapor generation in subcooled flow depends on local conditions and occurs at a heated surface⁶. No void data within the heated section were available as no probe or tap penetrations were found to be acceptable in designing the heaters.

In all power ramp tests, void was only seen in channel 3 (the annulus between the two heater tubes). Void was seen several seconds before flow instability and shutdown as shown in Figure 12. Table 1 shows how close OSV (channel exit) and flow instability are in terms of mockup heated section power. This result supports the SRS strategy of using OSV as a conservative but close predictor of flow instability.

CONCLUSIONS

A full scale rig mocking up the internals of an SRS reactor assembly has been successfully operated at prototypical power and flow to simulate hypothetical accidents. The behavior of the mockup led to the following conclusions.

- Flow instability was found to be a very sharp function of initial power during DEGB LOCA transients. Flow reduction and recovery were also very sensitive to power.
- OSV and overall FI in quasi-steady state power ramps were shown to be very close together in terms of assembly power. OSV was a conservative but close precursor of flow instability in this multichannel assembly.
- There was no propagation of void generation from one annular channel to neighboring channels in the quasi-steady state power ramp tests. OSV in one channel did not trigger immediate flow instability, nor did it cause immediate OSV elsewhere. Void generation was seen only in channel 3 in all of the power ramp tests.
- Void generation was always the first phenomenon to be seen in any test where conditions approached or exceeded those that cause flow instability. The mockup never experienced thermal excursion resulting from CHF as the first event in any test.

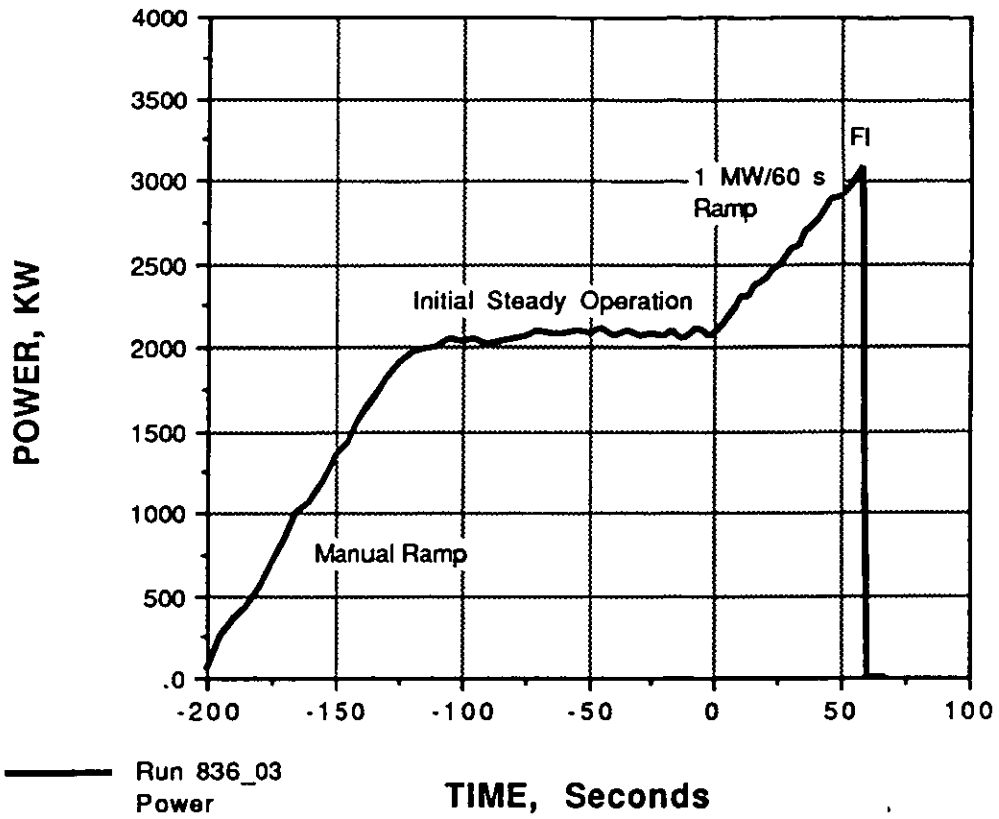


Figure 10. Example of a Power Ramp

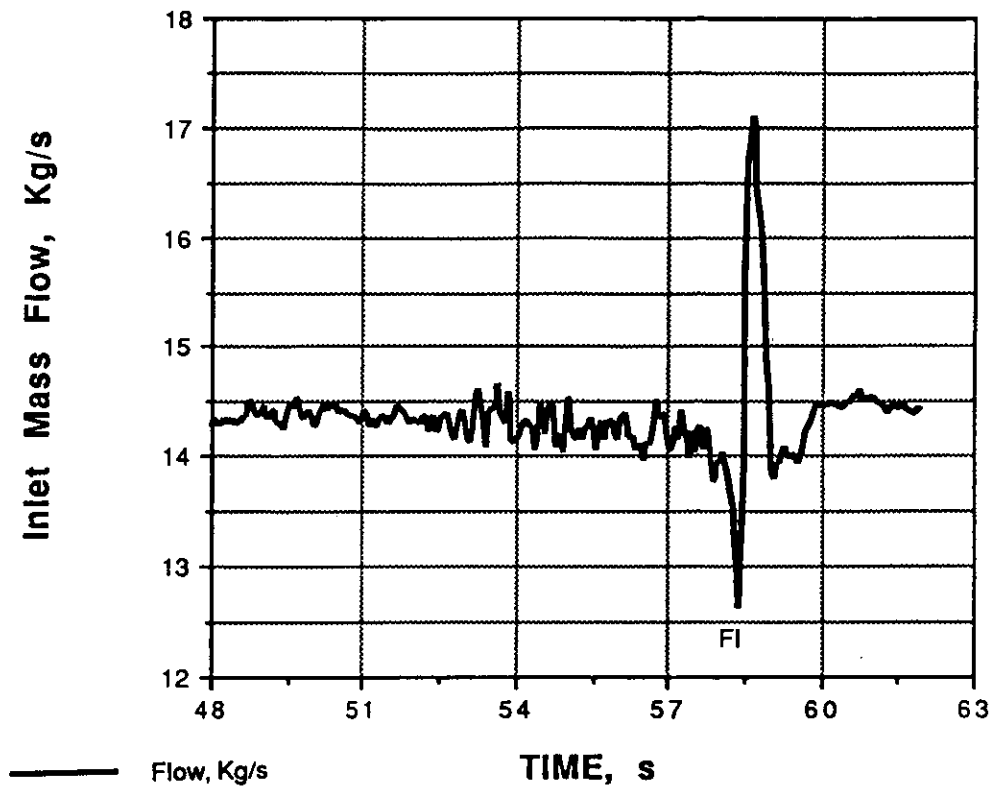


Figure 11. Inlet Mass Flow History Power Ramp Run 836-03

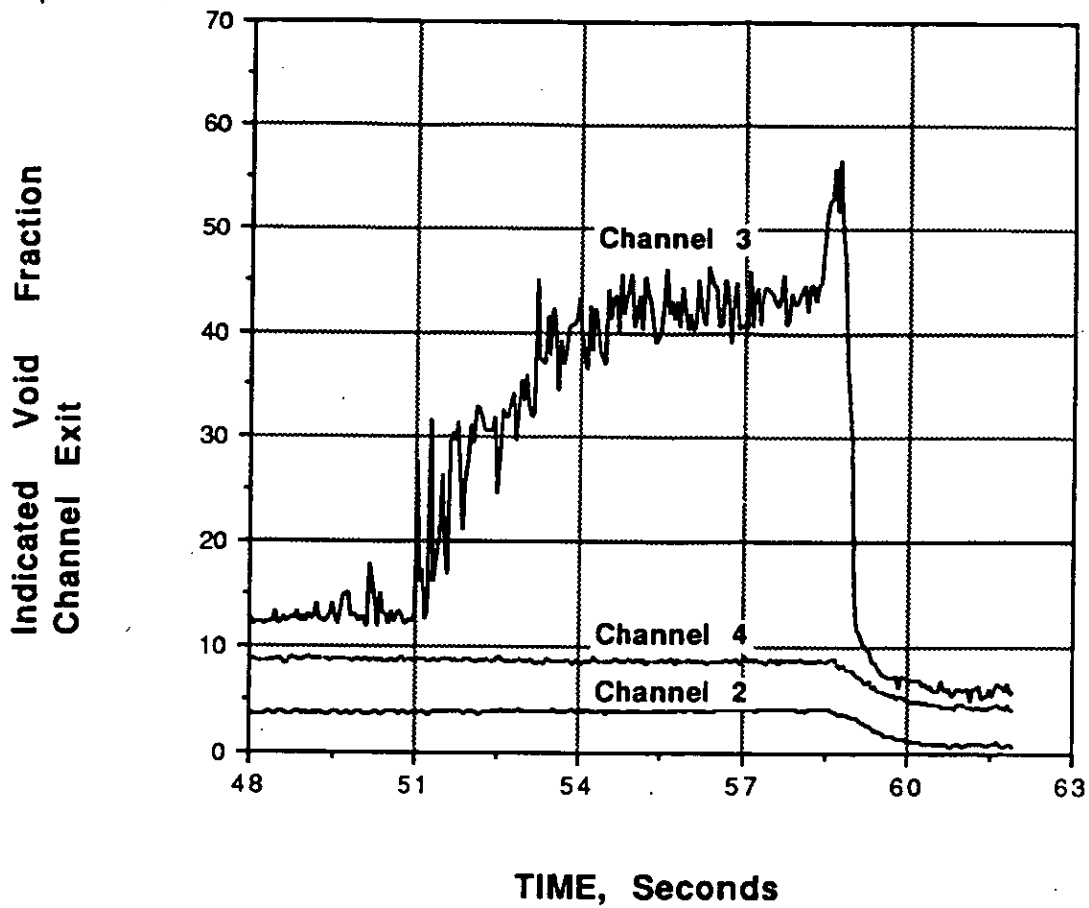


Figure 12. Void Fraction Data from Power Ramp Run 836-03

REFERENCES

1. M. LEDINEGG, "Instability of Flow During Natural and Forced Convection", *Die Wärme*, 61 891-898 (1938), Translation USAEC-tr-1861.
2. R. H. WHITTLE and R. FORGAN, "A Correlation for the Minima in the Pressure Drop Versus Flowrate Curves for Subcooled Water Flowing in Narrow Heated Channels", *Nuclear Engineering and Design*, 6, 89-99 (1967).
3. T. DOUGHERTY et. al., "Flow instability in Vertical Down-Flow at High Heat Fluxes", *Heat Transfer in High Energy/High Heat Flux Applications, HTD-Vol. 119*, 17-23, presented at the ASME 1989 Winter Annual Meeting, San Francisco, CA.
4. S. E. REED, J. W. BERTHOLD, and C. A. NASH, "Fiber Optic Void Fraction Sensor," *Proceedings of the IEEE Lasers and Electro-Optics Society Annual Meeting*, October 15-20, 1989, Orlando, FL.
5. R. T. LAHEY, Jr., "Two-Phase Flow Phenomena in Nuclear Reactor Technology", NUREG/CR-0580. Quarterly Progress Report no. 9 (June 1, 1978-August 31, 1978).
6. P. SAHA and N. ZUBER, "Point of Net Vapor Generation and Vapor Void Fraction in Subcooled Boiling", *International Heat Transfer Conference 5th Proceedings* (September 3-7, 1974).